

Dielectric Properties of Ethyleneglycol–1,4-Dioxane Mixtures Using TDR Method

Seiichi Sudo, Noriaki Oshiki, Naoki Shinyashiki,* and Shin Yagihara

Department of Physics, Tokai University, Kanagawa 259-1292, Japan

Ashok C. Kumbharkhane

School of Physical Sciences, Swami Ramanand Teerth Marathwada University, Nanded 431 606, India

Suresh C. Mehrotra

Department of Computer Science & Information Technology, Dr. B.A. Marathwada University, Aurangabad 431 004, India

Received: November 30, 2006; In Final Form: February 19, 2007

Complex permittivity has been determined for mixtures of ethyleneglycol–1,4-dioxane (EG–DX) with various concentrations in the frequency range from 100 MHz to 30 GHz at 25 °C by time domain reflectometry (TDR). A primary process with an asymmetric shape and a Debye-type small-amplitude high-frequency process are observed for each mixture. The deviation of the relaxation time for the primary process from that of the ideal mixture shows a maximum value at a mole fraction of 1,4-dioxane, $x_{\text{DX}} \cong 0.8$. The static permittivity for the mixtures can be explained using the Luzar model by assuming the formation of two types of hydrogen-bonded dimers, one between EG–EG (pair 1) and the other between EG–DX (pair 2). The number of these pairs is also estimated as a function of concentration. These results of the relaxation time and static permittivity are interpreted on the basis of a model of two kinds of cooperative domains coexisting in the mixtures.

Introduction

Dielectric studies have been carried out extensively on polyalcohol (molecule 1) and its water (molecule 2) mixtures to understand intra- and intermolecular interactions through hydrogen bonding.^{1–9} The dielectric parameters provide information about molecular dimers formed inside as a result of hydrogen bonding. In these systems, both components of the mixtures are polar and form hydrogen-bonded pairs. In principle, there will be three types of pairs (i.e., 1–1, 1–2, and 2–2). The Luzar model has been used to estimate the number of these dimers in the systems, in spite of the limitation that the model can only deal with two kinds of pairs. Therefore, this estimation will be more appropriate, if one component of the mixture is taken as a non-hydrogen-bonded liquid such as 1,4-dioxane (DX).

DX–alcohol mixtures have been investigated extensively by various techniques, such as those involving dielectrics, calorimetry, and viscosity.^{10–18} The dipole moment of the DX molecule is very small,¹⁹ and it is no pair formation between two DX molecules.²⁰ The interaction between DX molecules can be neglected for the DX–alcohol mixtures,²⁰ and the DX molecule induces hydrogen-bonded cleavage between alcohol molecules by adding DX to alcohol. Therefore, we can assume for the DX–alcohol mixture that two kinds of intermolecular hydrogen bonds exist: one is the hydrogen bond between alcohol molecules (pair 1) and the other is the hydrogen bond between alcohol and DX molecules (pair 2). In our earlier works, we performed dielectric measurements for 1-propanol–DX mixtures in the GHz region and discussed the cooperative motion of alcohol molecules.²¹ Furthermore, we also reported

the cluster size for pure water and methanol obtained from the results of the dielectric measurement for water– and methanol–DX mixtures.²²

The Kirkwood correlation factor determined from the dielectric constant gives information on the collective orientational correlation between molecules.²³ The deviation of the Kirkwood correlation factor from unity is a measure of the extent of intermolecular hydrogen bonding. The calculation of the theoretical dielectric constant using the Kirkwood correlation factor provides a more detailed theoretical model for mixtures. Luzar suggested a new theoretical model based on the mean field approximation for a hydrogen-bonded mixture,²⁴ and the theory gives a good qualitative agreement with the experimental results for dimethylsulphoxide–water mixtures. However, no further work has been carried out so far on alcohol systems using the Luzar model. In this work, ethyleneglycol–1,4-dioxane (EG–DX) mixtures with various concentrations are investigated by time domain reflectometry (TDR) in the frequency range between 100 MHz and 30 GHz at 25 °C. The dynamic behavior of the structure of the EG–DX mixtures is discussed on the basis of the Luzar model.

Experiments

The EG and DX were purchased from Aldrich. EG had more than 99.8% purity and contained less than 0.003% water. DX had more than 99.8% purity and contained less than 0.005% water. EG–DX mixtures with concentrations in the range from 100 to 0 wt % at 10 wt % intervals were prepared. The dielectric complex permittivity of the mixtures was measured by time domain reflectometry (TDR) in the frequency range between 100 MHz and 30 GHz at 25 °C. Details of the apparatus and the procedures of the TDR have been reported previously.^{5,26,27}

* Corresponding author.

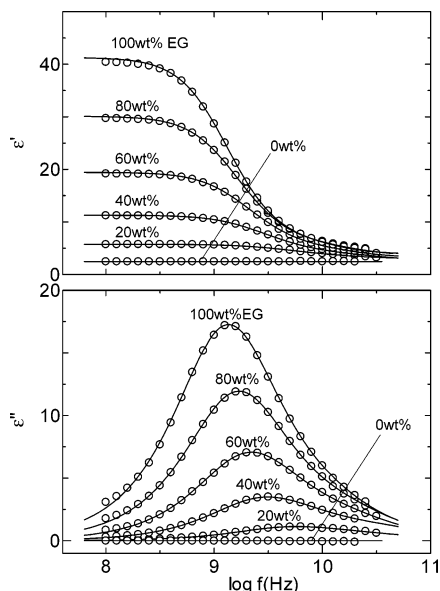


Figure 1. Frequency dependences of the dielectric constant and loss for ethyleneglycol-1,4-dioxane mixtures at various concentrations at 25 °C. Solid lines were calculated from the sum of the KWW and Debye equations.

Results

The frequency dependence of the dielectric constant and loss for 0, 20, 40, 60, 80, and 100 wt % EG–DX mixtures at 25 °C are shown in Figure 1. A single loss peak is clearly observed in the entire concentration range excepting pure DX. The loss-peak frequency of the EG–DX mixtures shifts to a lower frequency with increasing EG concentration and eventually reaches that for pure EG. The dielectric spectrum of the EG–DX mixtures shows good agreement with the relaxation curve obtained by the simple summation of the Kohlrausch–Williams–Watts (KWW)^{28,29} and Debye equations

$$\epsilon^*(\omega) = \epsilon_{\infty} + \Delta\epsilon_l \int_0^{\infty} \left[-\frac{d\Phi(t)}{dt} \right] \exp(-j\omega t) dt + \frac{\Delta\epsilon_h}{1 + j\omega\tau_h} \quad (1)$$

Here

$$\Phi(t) = \exp\left[-\left(\frac{t}{\tau_l}\right)^{\beta_K}\right] \quad (2)$$

where ϵ_{∞} is the limiting high-frequency permittivity, $\Delta\epsilon$ is the relaxation strength, τ is the relaxation time, ω is the angular frequency, and β_K ($0 < \beta_K \leq 1$) is a parameter for the asymmetrical broadness of the loss peak. The subscripts in eq 1 indicate the KWW-type low-frequency (l) and Debye-type high-frequency (h) processes. The static dielectric constant is written as $\epsilon_0 = \Delta\epsilon_l + \Delta\epsilon_h + \epsilon_{\infty}$.

Figure 2 shows the dependence of the mole fraction of DX, x_{DX} , on the dielectric relaxation parameters for the EG–DX mixtures. The dielectric relaxation time of the low-frequency process decreases with increasing x_{DX} , and it does not depend linearly on x_{DX} . The relaxation time of the high-frequency process is independent of x_{DX} . The relaxation strength of the low-frequency process decreases with increasing x_{DX} . The relaxation strength of the high-frequency process is independent of x_{DX} for $x_{DX} < 0.6$, and decreases with increasing x_{DX} for $x_{DX} > 0.6$. The value of β_K decreases with increasing x_{DX} over the whole concentration range measured.

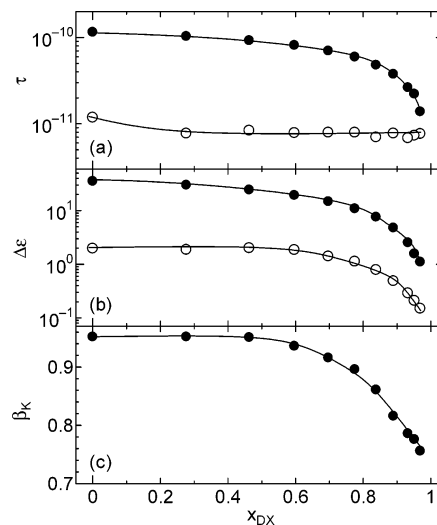


Figure 2. Mole fraction dependence of (a) relaxation time, (b) relaxation strength, and (c) broadness of the relaxation curve for ethyleneglycol-1,4-dioxane mixtures at 25 °C. Closed and open circles indicate the low- and high-frequency processes, respectively.

Discussion

Dielectric measurements up to the sub-THz and THz regions have been performed for water, monohydric alcohol, ethyleneglycol, and alcohol–water mixtures around room temperature, and some relaxation processes have been observed in the frequency range higher than the primary loss-peak frequency.^{30–35} The amplitudes of these high-frequency processes are much lower than that of the primary process. The relaxation times of these high-frequency processes are 1–2 decades smaller than that of the primary process. In one of the models of the molecular mechanism, the high- and middle-frequency processes are due to the rotation of non-hydrogen-bonded OH groups around the C–OH bond and non-hydrogen-bonded alcohol molecules.^{30,31} Our experimental results for the EG–DX mixtures suggest that the KWW-type primary and the small-amplitude Debye-type high-frequency processes are observed in the whole frequency range measured. The dielectric relaxation parameters of the primary process strongly depend on the EG concentration. It is expected that this primary process is due to the cooperative motion of EG–EG and/or EG–DX molecules through hydrogen bonds. On the other hand, our results for the dielectric parameters of the Debye-type high-frequency process have large errors, because of the occurrence of relaxation processes above the high-frequency limit of our measurement. Therefore, we mainly focus on the concentration dependence of the dielectric parameters of the primary process and discuss the local structure of the EG–DX mixtures using a cooperative domain model, which explains the local structure for alcohol–water mixtures.⁹ Furthermore, the number of hydrogen bonds of EG–EG and EG–DX molecules are calculated using the Luzar model, and the local structure, based on the number of hydrogen bonds, is discussed.²⁴

Generally, the primary process observed for various glass-forming polymers, associated liquids, and those water mixtures exhibits an asymmetric loss peak. In a theoretical study, it has been suggested that the motional units in the correlated domains cooperatively move and the heterogeneity of the distribution of the size of the domain results in the asymmetric shape of the loss peak.³³ We have already reported that the asymmetric shape of the loss peak for alcohol–water mixtures is due to the heterogeneous structure, reflecting the variation of the size and

the dynamical structure of a cooperative domains (CDs).⁹ A CD is defined as a domain in which the reorientation of molecules cooperatively occurs with dipole correlations. Then, the cooperative motion is characterized by the size and the structure of the CD. Stronger interactions among moving units can yield a large CD, and a variation of the size of the CD results in a corresponding variation of the microscopic relaxation time; this variation of microscopic relaxation time causes an asymmetric dielectric loss peak. We assumed that three kinds of intermolecular interactions existed in the alcohol–water mixtures.^{9,34–37} One is the interaction between the alcohol molecules. The second is the interaction between the water molecules. The last one is the interaction between the alcohol and water molecules. The molecules form CDs based on the three kinds of molecular interactions, and the coexistence of three kinds of CDs leads to the asymmetric shape of the loss peak for the alcohol–water mixtures. The populations of the CDs under the three kinds of interactions strongly depend on the concentration, and the coexistence of the three kinds of CDs can be used to explain the concentration dependence of the relaxation time and its distribution for the alcohol–water mixtures. We assumed that the interaction between DX molecules can also be neglected for the EG–DX mixtures; thus, two kinds of CDs exist in the EG–DX mixtures. We discuss the concentration dependence of the dielectric relaxation parameters on basis of the coexistence of the two kinds of CDs. CD_{EG} includes only EG molecules, and CD_{EG-DX} includes both EG and DX molecules.

Relaxation Time. The relaxation time is related to the apparent activation free energy of the rearrangement of dipoles by the Eyring formula³⁸

$$\tau = \frac{h}{k_B T} \exp\left(\frac{\Delta G}{RT}\right) \quad (3)$$

Here, h is Planck constant, k_B is the Boltzmann constant, T is the absolute temperature, R is the gas constant, and ΔG is the apparent activation free energy. Assuming an ideal mixture of liquid 1 and liquid 2, in which the dynamical structure of each pure liquid is retained in a mixed environment and the free energy of the mixed environment is equal to the arithmetical mean of the free energies of the pure liquids, the apparent activation free energy, ΔG_{mix} , is given by³⁹

$$\Delta G_{\text{mix}} = x_1 \Delta G_1 + (1 - x_1) \Delta G_2 \quad (4)$$

where ΔG_1 and ΔG_2 are the apparent activation free energies for liquid 1 and liquid 2, respectively, and x_1 is the mole fraction of liquid 1. Then, the ideal behavior of the relaxation time, τ_{ideal} , for the mixture is given by

$$\tau_{\text{ideal}} = \frac{h}{kT} \exp\left(\frac{\Delta G_{\text{mix}}}{RT}\right) = \tau_1^{x_1} \tau_2^{(1-x_1)} \quad (5)$$

If ΔG_{mix} is given by the three kinds of free energies ΔG_1 , ΔG_2 , and ΔG_{12} , where ΔG_{12} is the apparent activation free energy of the mixed environment of molecules of liquid 1 and liquid 2, and ΔG_{12} is equal to the arithmetical mean of the free energies of the pure liquids. Then, the relaxation time can be described using eq 5. When ΔG_{12} is not equal to the arithmetical mean of the free energies of the pure liquids, the observed relaxation time disagrees with eq 5.

According to eq 5, the ideal behavior of the relaxation time, τ_{ideal} , for the EG–DX mixtures is calculated. Here, the subscripts 1 and 2 in eq 4 and 5 denote DX and EG, and ΔG_{DX} and ΔG_{EG}

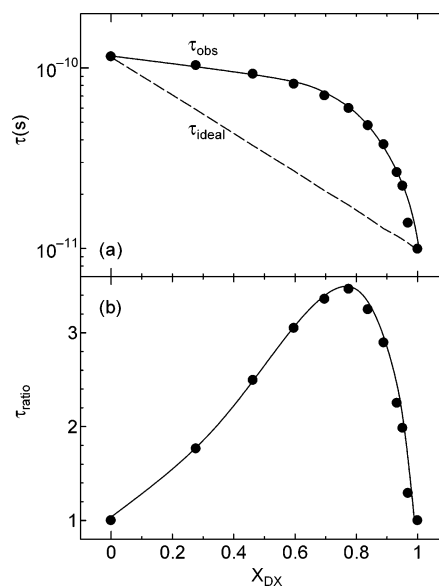


Figure 3. (a) Mole fraction dependence of the relaxation time of the low-frequency process, τ_{obs} , for ethyleneglycol-1,4-dioxane mixtures at 25 °C. The dashed line shows the behavior for the ideal mixture. (b) Mole fraction dependence of τ_{ratio} for ethyleneglycol-1,4-dioxane mixtures. τ_{ratio} is defined as the ratio of the observed relaxation time to that relaxation time of the ideal mixture, τ_{ideal} .

are the apparent activation free energies of the rearrangements of CD_{DX} and CD_{EG} , respectively. The plots of the logarithm of τ_{ideal} against the mole fraction of DX show a linear dependence, according to this equation, when the EG–DX mixtures are ideal. We must estimate the relaxation time of pure DX to calculate τ_{ideal} for EG–DX mixtures, because the relaxation process of pure DX was not observed. The early Debye theory, in which a relaxation process is explained as being due to the hindered reorientation of spherical polar molecules, predicts the proportionality between the relaxation time and the viscosity as⁴⁰

$$\tau = \frac{4\pi a^3}{k_B T} \eta \quad (6)$$

Here, a is the radius of a single molecule and η is the viscosity. We performed the dielectric measurement for 1,3-dioxane (13DX) using a TDR measuring system and the viscosimetry for 13DX and DX using an Ubbelohde capillary viscosimeter at 25 °C. The dielectric relaxation time for 13DX is 9.0 ps. The viscosity of 13DX is $1.0837 (\pm 0.008)$ cp, and that of DX is $1.1971 (\pm 0.0004)$ cp at 25 °C. Assuming that the radius of a DX molecule equals that of a 13DX molecule, the relaxation time for pure DX is estimated as $\tau_{DX} = 7.2$ ps by eq 6. This value agrees with the extrapolation of the relaxation time of the primary process for the EG–DX mixtures, as shown in Figure 2a. The values of τ_{ideal} for the EG–DX mixtures are calculated from the observed value of τ_{EG} and the estimated value of τ_{DX} . The observed relaxation time, τ_{obs} , and the ideal relaxation time obtained from eq 6, τ_{ideal} , are shown by closed circles and a dashed line in Figure 3a, respectively. The τ_{obs} does not agree with τ_{ideal} over the entire concentration range. τ_{ratio} is defined as the ratio $\tau_{\text{obs}}/\tau_{\text{ideal}}$ to discuss the deviation of τ_{obs} from τ_{ideal} . Figure 3b shows the plots of τ_{ratio} against x_{DX} . The value of τ_{ratio} shows a maximum at $x_{DX} \approx 0.8$.

The disagreement between τ_{obs} and τ_{ideal} reflects the apparent activation free energy for the rearrangement of CD_{EG-DX} . The existence of the CD_{EG-DX} leads to the deviation of the x_{DX} dependence of the relaxation time from linearity. The maximum

value of τ_{ratio} at $x_{\text{DX}} \cong 0.8$ indicates that the population of $\text{CD}_{\text{EG-DX}}$ is a maximum at this concentration.

Dielectric Constant. The Kirkwood correlation factor g_i for a mixture can be expressed as²⁴

$$\frac{(\epsilon_0 - \epsilon_\infty)(2\epsilon_0 + \epsilon_\infty)}{9\epsilon_0} = \frac{4\pi}{9kT} \sum_{i=1}^2 g_i \rho_i \mu_i^2 \quad (7)$$

where $i = 1$ and 2 represent EG and DX, respectively. Here, μ_i is the dipole moment of an EG or DX molecule, ρ_i is the density, and g_i is the Kirkwood correlation factor for the i th liquid component. The interpretation of the dielectric phenomena in terms of the Kirkwood correlation factor is very difficult for a mixture of associated compounds. It is impossible to separate the average correlation factors g_1 and g_2 from a single value of the static dielectric constant without any assumptions. Kirkwood–Fröhlich theory must be applied to media containing two species of molecules, and the cross-correlation terms must be taken into account to separate g_1 and g_2 when considering only the hydrogen-bond contribution to the dipole–dipole correlation. In the present approach, the Kirkwood correlation factors for individual species $i = 1$ and 2 are modified, and these new correlations are described by the following relations:²⁴

$$g_1 = 1 + Z_{11} \cos \varphi_{11} + Z_{12} \cos \varphi_{12} (\mu_2/\mu_1) \quad (8)$$

$$g_2 = 1 + Z_{21} \cos \varphi_{21} (\mu_1/\mu_2) \quad (9)$$

where $Z_{11} = 2\langle n_{\text{HB}}^{11} \rangle$, $Z_{12} = \langle n_{\text{HB}}^{12} \rangle$, and $Z_{21} = \langle n_{\text{HB}}^{12} \rangle (1 - x_{\text{DX}})/x_{\text{DX}}$ are the average numbers of hydrogen bonds between EG–EG, EG–DX, and DX–EG pairs, respectively. φ_{11} , φ_{12} , and φ_{21} are the average angles between neighboring dipoles of EG–EG, EG–DX, and DX–EG pairs, respectively, and $\cos \varphi_{ij}$ is taken to be $1/3$. The average number of hydrogen bonds [$\langle n_{\text{HB}}^{11} \rangle$, $\langle n_{\text{HB}}^{12} \rangle$, and $\langle n_{\text{HB}}^{21} \rangle$] per EG molecule for li pairs ($i = 1$ or 2) has been determined using to the following relation:²⁴

$$\langle n_{\text{HB}}^{li} \rangle = n_i \omega^{li} / n_1 \quad (10)$$

where $\omega^{li} = 1/[1 + \alpha^{li} \exp(\beta E^{li})]$ is the probability of bond formation between EG and DX. n_i is the number density of EG molecules, $\beta = 1/kT$, and α^{li} are the statistical volume ratios of the two subvolumes of the phase space related to the non-hydrogen-bonded and hydrogen-bonded pairs. These hydrogen-bonded pairs have only two energy levels, E^{11} and E^{12} , for 11 and 12 pair-formed bonds, respectively. The values of $\langle n_{\text{HB}}^{11} \rangle$ and $\langle n_{\text{HB}}^{12} \rangle$ depend on the number densities of the hydrogen-bonded pairs between EG and DX (n_{12}) and between EG molecules ($n_{11} = 2n_1 - n_{12}$), respectively. These can be calculated, during which EG–EG (11 pair) and EG–DX (12 pair) are formed.²⁴

The concentration dependence of the static dielectric constants is calculated using eqs 7–10 and is compared with experimental data. Here, the parameters required in eqs 7–10 are the dipole moments of molecules EG, μ_{EG} , and DX, μ_{DX} , calculated from the Onsager relation,²⁴ and the refractive index, n , calculated from the Lorenz–Lorenz equation.^{24,25} The polarizability, static volume ratio, number of hydrogen bonds, and bonding energy are the fitting parameters. The model gives a good qualitative account of the dielectric constant of the EG–DX mixtures. In our analysis, the best possible values of molecular parameters with which the theoretical static dielectric constant values are in reasonable agreement with the experimental values, shown in Figure 4, are given in Table 1, and the fitting parameters

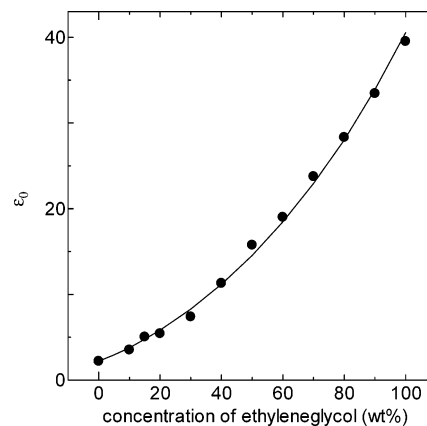


Figure 4. Plots of the static dielectric constant against concentration of ethyleneglycol for ethyleneglycol-1,4-dioxane mixtures. The solid line is calculated by eq 7, and here, Kirkwood correlation factors are calculated from the Luzar model.

TABLE 1: Molecular Parameters Used in Computation of the Static Dielectric Constants

dipole moment of EG in Debye, μ_1	= 2.38 D
dipole moment of DX in Debye, μ_2	= 0.97 D
polarizability for EG in \AA^3	= 5.90
polarizability of DX in \AA^3	= 2.84
bonding energy for EG–EG, E^{11}	= -15.80 kJ/mol
bonding energy for EG–DX, E^{12}	= -16.79 kJ/mol
statistical volume ratio for EG–EG, α^{11}	= 28
statistical volume ratio for EG–DX, α^{12}	= 28
number of hydrogen bonds of EG	= 2

obtained are nearly the same as those for DMSO–water mixtures given in ref 24. Figure 5, panels a and b, shows plots of the correlation factor and the average number of hydrogen bonds of EG–EG molecules (11 pairs) and EG–DX molecules (12 pairs) per EG molecule against x_{DX} for the EG–DX mixtures. g_1 and g_2 decrease with increasing x_{DX} , whereas n_{HB}^{11} decreases and n_{HB}^{12} increases with increasing x_{DX} . The value of n_{HB}^{11} is 1.91 at $x_{\text{DX}} = 0$, and that of n_{HB}^{12} is 1.93 at $x_{\text{DX}} = 1$. These results suggest that one EG molecule interacts with 1.9 surrounding EG molecules by hydrogen bonding in pure EG. We calculated the average number of hydrogen-bonded EG–EG pairs, $[n_{\text{HB}}^{11}]_V$, and EG–DX pairs, $[n_{\text{HB}}^{12}]_V$, per unit volume ($/\text{cm}^3$) using

$$[n_{\text{HB}}^{11}]_V = \frac{C_{\text{EG}} \rho_{\text{mix}} N_A}{M_{\text{EG}}} n_{\text{HB}}^{11} \quad (/ \text{cm}^3)$$

and

$$[n_{\text{HB}}^{12}]_V = \frac{C_{\text{EG}} \rho_{\text{mix}} N_A}{M_{\text{EG}}} n_{\text{HB}}^{12} \quad (/ \text{cm}^3) \quad (11)$$

Here, C_{EG} is the weight fraction of EG, ρ_{mix} (g/cm^3) is the density of the mixtures, N_A is the Avogadro number, as 6.02×10^{23} ($/\text{mol}$), and M_{EG} is the molecular weight of EG. Figure 6 shows plots of $[n_{\text{HB}}^{11}]_V$ and $[n_{\text{HB}}^{12}]_V$ against x_{DX} . The value of $[n_{\text{HB}}^{11}]_V$ decreases with increasing x_{DX} , and that of $[n_{\text{HB}}^{12}]_V$ has a maximum at $x_{\text{DX}} \cong 0.8$; this concentration agrees with the concentration at which τ_{ratio} shows a maximum value.

Local Structure of EG–DX Mixtures. We discuss the concentration dependence of the population of two kinds of CDs for the EG–DX mixtures. According to the cooperative domain model, the pure EG must contain only CD_{EG} , because no DX

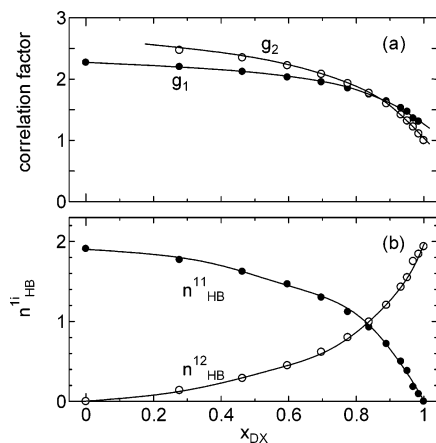


Figure 5. Plots of (a) the correlation factor and (b) the number of hydrogen-bonded per ethyleneglycol molecule against mole fraction of 1,4-dioxane for ethyleneglycol–1,4-dioxane mixtures.

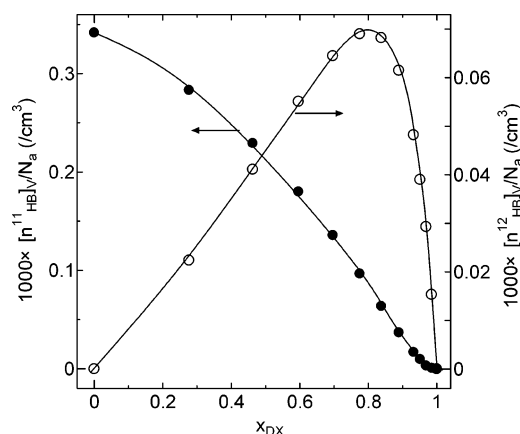


Figure 6. Plots of the number of hydrogen bonds per unit volume against mole fraction of 1,4-dioxane for ethyleneglycol–1,4-dioxane mixtures.

molecules are added. In this case, the β_K value is not unity, which is reflected in the microscopic relaxation time distribution of CD_{EG} , and the size of CD_{EG} is heterogeneous. At $0 < x_{DX} < 0.8$, DX molecules interact with surrounding EG molecules by hydrogen bonding, and these molecules form CD_{EG-DX} . The fraction of CD_{EG-DX} increases, and that of CD_{EG} decreases with increasing x_{DX} . Then, the increase in the population of CD_{EG-DX} brings about an increase in the heterogeneity of the CD size, which leads to a decrease in β_K . At around $x_{DX} = 0.8$, the average size of CD_{EG-DX} and the average number of hydrogen bonds between EG and DX molecules are maximum, because τ_{ratio} and $[n_{HB}^{i2}]_V$ are maximum. For $0.8 < x_{DX}$, the decrease in the number of EG molecules with increasing x_{DX} leads to a decrease in the average number of hydrogen bonds between EG and DX molecules, which is reflected in the decrease in the fraction of CD_{EG-DX} . The concentration $x_{DX} \approx 1$ can be interpreted as the environment of infinitely diluted EG. One EG molecule forms hydrogen bonds with about two DX molecules, and these molecules form one CD_{EG-DX} at this concentration, because $n_{HB}^{i2} \approx 2$. The value of n_{HB}^{i2} at $x_{DX} \approx 1$ implies that one EG molecule in a DX environment forms hydrogen bonding with about two DX molecules, and n_{HB}^{i2} cannot exceed 2 in a mixed environment of DX and EG. Thermal analysis measurements of EG–DX mixtures have been performed, and the excess activation free energy of the EG–DX mixtures compared with the ideal mixture shows a minimum at $x_{DX} \approx 0.6$, and this concentration corresponds to the binary composition of a 1 EG–2 DX complex.¹⁶ This description

corresponds with our results for the size of the cooperative domain in infinitely diluted EG.

Finally, the application of the Luzar model is discussed. The concentration at which n_{HB}^{i2} shows a maximum obtained using the Luzar model is in good agreement with the concentration at which τ_{ratio} shows a maximum. This agreement suggests that the physical picture obtained from the Luzar model using the dielectric constant does not contradict that obtained from the cooperative domain model using the relaxation time. Therefore, the Luzar model provides a theoretical basis for the computation of the molecular parameters, as listed in Table 1, with the help of experimental values of the static dielectric constant in the binary liquid mixture. There is no other theory available that provides these molecular parameters.

Conclusion

The asymmetric shape of the loss peak is observed for the EG–DX mixtures over the entire concentration range. The concentration dependence of the relaxation time of the primary process deviates from that expected for the ideal mixture. The existence of CD_{EG-DX} leads to this deviation of relaxation time, which shows a maximum at $x_{DX} \approx 0.8$. On the other hand, the numbers of hydrogen bonds of EG–EG and EG–DX molecules are obtained from the dielectric constant using the Luzar model. On average, one EG molecule forms hydrogen bonds 1.9 surrounding EG molecules in pure EG. The number of hydrogen bonds of EG–DX molecules increases with increasing DX concentration and is a maximum at $x_{DX} \approx 0.8$. The hydrogen bonds between EG and DX molecules results in the formation of CD_{EG-DX} . The concentration of $x_{DX} \approx 0.8$ agrees precisely with the concentration at which the relaxation time deviates most from that of the ideal mixture.

Acknowledgment. This work was partly supported by the Ministry of Education, Science, Sports and Culture, Grant-in-Aid for Specially Promoted Research (18031034).

References and Notes

- (1) Wang, F.; Pottel, R.; Kaatze, U. *J. Phys. Chem. B* **1997**, *101*, 922.
- (2) Gestblom, B.; Sjöblom, J. *J. Phys. Chem.* **1986**, *90*, 4175.
- (3) Paduano, L.; Sartori, R.; D'Errico, G.; Vitagliano, V. *J. Chem. Soc. Faraday Trans.* **1998**, *94*, 2571.
- (4) Bao, J.; Swicord, M. L.; Davis, C. C. *J. Chem. Phys.* **1996**, *104*, 4441.
- (5) Mashimo, S.; Umehara, T.; Redlin, H. *J. Chem. Phys.* **1991**, *95*, 6257.
- (6) Mashimo, S.; Kuwabara, S.; Yagihara, S.; Higasi, K. *J. Chem. Phys.* **1989**, *90*, 3292.
- (7) Shinyashiki, N.; Sudo, S.; Abe, W.; Yagihara, S. *J. Chem. Phys.* **1998**, *109*, 9843.
- (8) Schwerdtfeger, S.; Köhler, F.; Pottel, R.; Kaatze, U. *J. Chem. Phys.* **2001**, *115*, 4186.
- (9) Sudo, S.; Shinyashiki, N.; Kitsuki, Y.; Yagihara, S. *J. Phys. Chem. A* **2002**, *106*, 458.
- (10) Papanastasiou, G. E.; Papoutsis, A. D.; Kokkinidis, G. I. *J. Chem. Eng. Data* **1987**, *32*, 377.
- (11) Anderson, J. E. *J. Phys. Chem.* **1991**, *95*, 7062.
- (12) Corradini, F.; Marcheselli, L.; Tassi, L.; Tosi, G. *Bull. Chem. Soc. Jpn.* **1993**, *66*, 1886.
- (13) Orttung, W. H.; Sun, T. C.; Kin, J. M.; Kehman, J.; Kalifé, L. L. *J. Phys. Chem.* **1993**, *97*, 5384.
- (14) Corradini, F.; Marchetti, A.; Tagliuzucchi, M.; Tassi, L.; Tosi, G. *Aust. J. Chem.* **1994**, *47*, 1117.
- (15) Aminabhavi, T. M.; Gopalakrishna, B. *J. Chem. Eng. Data* **1995**, *40*, 856.
- (16) Corradini, F.; Marchetti, A.; Tagliuzucchi, M.; Tassi, L.; Tosi, G. *Aust. J. Chem.* **1995**, *48*, 1193.
- (17) Aralaguppi, M. I.; Jadar, C. V.; Aminabhavi, T. M. *J. Chem. Eng. Data* **1996**, *41*, 1307.
- (18) Contreras, S. M. *J. Chem. Eng. Data* **2001**, *46*, 1149.

- (19) McClellan, A. L. *Table of Experimental Dipole Moments*; W. H. Freeman & Co.: San Francisco, CA, 1966.
- (20) Tominaga, Y.; Takeuchi, S. M. *J. Chem. Phys.* **1996**, *104*, 7377.
- (21) Yagihara, S.; Nozaki, R.; Mashimo, S.; Higasi, K. *Chem. Lett.* **1985**, *1*, 137.
- (22) Mashimo, S.; Miura, N.; Umehara, T.; Yagihara, S.; Higasi, K. *J. Chem. Phys.* **1992**, *96*, 6358.
- (23) Kirkwood, J. G. *J. Chem. Phys.* **1939**, *7*, 911.
- (24) Luzar, A. *J. Mol. Liq.* **1990**, *46*, 221.
- (25) Bottcher, J. F. *Theory of Electric Polarization*; Elsevier: Amsterdam, 1973; Vol. I.
- (26) Mashimo, S.; Miura, N.; Umehara, T.; Yagihara, S.; Higasi, K. *J. Chem. Phys.* **1992**, *96*, 6358.
- (27) Mashimo, S.; Miura, N. *J. Chem. Phys.* **1993**, *99*, 9874.
- (28) Kohlrausch, R. *Prog. Ann. Phys.* **1854**, *91*, 179.
- (29) Williams, G.; Watts, D. C. *Trans. Faraday Soc.* **1971**, *66*, 80.
- (30) Garg, K. S.; Smyth, C. P. *J. Phys. Chem.* **1965**, *69*, 1294.
- (31) Barthel, J.; Bachhuber, K.; Buchner, R.; Hetzenauer, H. *Chem. Phys. Lett.* **1990**, *165*, 369.
- (32) Kaatze, U.; Behrends, R.; Pottel, R. *J. Non-Cryst. Solids* **2002**, *305*, 19.
- (33) Fukasawa, T.; Sato, T.; Watanabe, J.; Hama, Y.; Kunz, W.; Buchner, R. *Phys. Rev. Lett.* **2005**, *95*, 197802.
- (34) Bertolini, D.; Cassettari, M.; Ferrari, C.; Tombari, E. *J. Chem. Phys.* **1998**, *108*, 6416.
- (35) Sudo, S.; Shimomura, M.; Shinyashiki, N.; Yagihara, S. *J. Non-Cryst. Solids* **2002**, *307–310*, 356–363.
- (36) Sudo, S.; Shimomura, M.; Saito, T.; Kasiwagi, T.; Shinyashiki, N.; Yagihara, S. *J. Non-Cryst. Solids* **2002**, *305*, 197–203.
- (37) Sudo, S.; Shimomura, M.; Tsubotani, S.; Shinyashiki, N.; Yagihara, S. *J. Chem. Phys.* **2004**, *121*, 7332.
- (38) Hill, N. E.; Vaughan, W. E.; Price, A. H.; Davies, M. *Dielectric Properties and Molecular Behaviour*; Reinhold: London, 1969.
- (39) Bertolini, D.; Cassettari, M.; Ferrari, C.; Tombari, E. *J. Chem. Phys.* **1998**, *108*, 6416.
- (40) Franks, F. *The Physics and Physical Chemistry of Water*; Plenum: New York, 1972; Chapter 7.